Asymmetric dynamic behaviors of magnetic domain wall in trapezoid-cross-section nanostrip*

Xiao-Ping Ma(马晓萍)[1], Hong-Guang Piao(朴红光)[1,†], Lei Yang(杨磊)[1], Dong-Hyun Kim[2], Chun-Yeol You[3], and Liqing Pan(潘礼庆)[1]

[1] Research Institute for Magnetoelectric & Weak Magnetic-field Detection, College of Science, China Three Gorges University, Yichang 443002, China
[2] Department of Physics, Chungbuk National University, Cheongju 28644, Chungbuk, Republic of Korea
[3] Department of Emerging Materials Science, Daegu Gyeongbuk Institute of Science and Technology (DGIST), Daegu 42988, Republic of Korea

(Received 27 March 2020; revised manuscript received 1 June 2020; accepted manuscript online 29 June 2020)

Field-driven magnetic domain wall propagation in ferromagnetic nanostrips with trapezoidal cross section has been systematically investigated by means of micromagnetic simulation. Asymmetric dynamic behaviors of domain wall, depending on the propagation direction, were observed under an external magnetic field. When the domain walls propagate in the opposite direction along the long axis of the nanostrip, the Walker breakdown fields as well as the average velocities are different. The asymmetric landscape of demagnetization energies, which arises from the trapezoidal geometry, is the main origin of the asymmetric propagation behavior. Furthermore, a trapezoid-cross-section nanostrip will become a nanotube if it is rolled artificially along its long axis, and thus a two-dimensional transverse domain wall will become a three-dimensional one. Interestingly, it is found that the asymmetric behaviors observed in two-dimensional nanostrips with trapezoidal cross section are similar with some dynamic properties occurring in three-dimensional nanotubes.

Keywords: ferromagnetic nanowire, magnetic domain wall, geometric effect, asymmetric Walker breakdown

PACS: 75.75.–c, 75.78.–n, 75.78.Cd, 75.78.Fg **DOI:** 10.1088/1674-1056/aba09a

1. Introduction

Control and understanding of the magnetic domain wall (DW) motion are essential for future realization of spintronic devices, such as DW logic circuits and DW memories.[1–4] With the development of lithography techniques, the DW dynamic behavior can be confined and manipulated on various patterned ferromagnetic nanowires, such as nanostrip, nanotube, and nanocylinder. Many works have shown that the propagating DW dynamics is significantly affected by the nanowire geometries and dimensions,[5–9] e.g., the edge roughness of nanowires can be used to improve the DW dynamic behavior by suppressing the Walker breakdown phenomenon.[10–14] The Walker breakdown causes an abrupt change of the DW structure above a critical field, and consequently influences the DW speed and propagation stability.

On the other hand, the lithography technique has problems, more or less, with fabrication of sharp edges. Thus the so-called rectangular cross section is roughly D-shaped or trapezoidal.[15,16] Concerning about the actual situation, it is essential to investigate the DW dynamic behavior in nanowires with no sharply shaped edges. In addition, a trapezoid-cross-section nanostrip will become a nanotube if it is rolled artificially along its long axis, and thus a two-dimensional transverse DW will become a three-dimensional DW. As it will be unveiled later, the dynamic properties of a DW in trapezoid-cross-section nanostrip behaves similarly as it in a three-dimensional nanotube. The asymmetric dynamic behaviors in such as the asymmetric energy landscape[17] and the different Walker breakdown field[14,18] have been reported when the DW propagates in a nanotube. However, little is known about the dynamic correlation between the two-dimensional and three-dimensional transverse DW.[19] Furthermore, for the reason of easy fabrication, magnetic nanostrips are currently the most common choice in applications in such as DW guides. In this work, with changing of the external magnetic field strength as well as switching of the field direction, DW dynamic behaviors are investigated in ferromagnetic nanostrips with trapezoidal cross section.

2. Micromagnetic simulations

To investigate the propagation direction dependent asymmetric dynamic behaviors of a DW, the micromagnetic simulations were performed by Mumax3,[20] which describes the magnetization evolution by solving the Landau–Lifshitz–Gilbert equation[21]

$$\frac{\mathrm{d}\boldsymbol{M}}{\mathrm{d}t} = -|\gamma|\boldsymbol{M}\times\boldsymbol{H}_{\mathrm{eff}} + \frac{\alpha}{M_{\mathrm{s}}}\boldsymbol{M}\times\frac{\mathrm{d}\boldsymbol{M}}{\mathrm{d}t},$$

where $\boldsymbol{M}$ is the magnetization, M_{s} is the saturation magnetization, $\boldsymbol{H}_{\mathrm{eff}}$ is the effective magnetic field, γ is the gyromagneic ratio, and α is a phenomenological damping parameter.

*Project supported by the National Key R&D Program of China (Grant Nos. 2017YFB0903700 and 2017YFB0903702), Yichang Government Fund (Grant No. A19-402-a05), the Korea Research Foundation (NRF) (Grant No. 2018R1A2B3009569), and Korea Basic Science Institute (KBSI) (Grant No. D39614).

†Corresponding author. E-mail: hgpiao@ctgu.edu.cn

The strength of the external magnetic field (H_{ext}) was changed from 10 Oe to 50 Oe. The length of the nanostrip is fixed at 6000 nm, and thickness h varies from 5 nm to 8 nm. The bottom length of cross section is fixed at 50 nm, and the value a varies from 5 nm to 10 nm to change the slope of both edges of the nanostrip, as shown in Fig. 1. Here material parameters of permalloy were considered with the exchange stiffness coefficient of $A_{ex} = 13 \times 10^{-12}$ J/m, the saturation magnetization of $M_s = 8.6 \times 10^5$ A/m, and zero magnetocrystalline anisotropy. In all the simulations, the unit cell dimension of $2 \times 1 \times 2$ nm^3 and the Gilbert damping constant of $\alpha = 0.01$ were used. To smooth the edge, the cell at the geometry edge is further divided into $8 \times 8 \times 8 = 512$ small ones. Before applying the external magnetic field, a head-to-head transverse DW has been initially positioned at the center of ferromagnetic nanostrip.

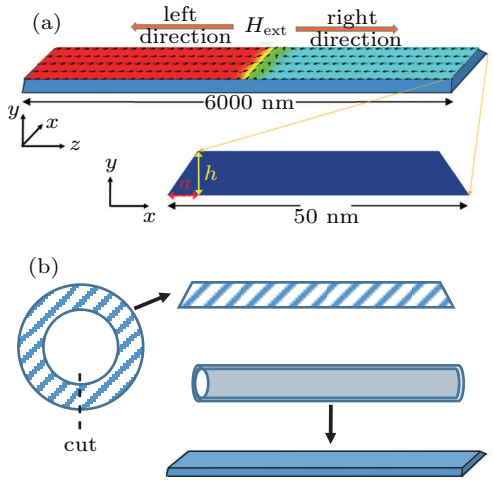

Fig. 1. (a) The geometry and dimension of the trapezoid-cross-section nanostrip. The external magnetic field direction is denoted by the arrows on the top. A head-to-head transverse DW is initially positioned in the center of the nanostrip, and its direction is denoted by the arrows inside. The cross section of the nanostrip is shown at the bottom. (b) The schematic diagrams of the nanotube unrolled into a trapezoid-cross-section nanostrip when it is cut along the long axis.

3. Results and discussion

After energy relaxation process, a series of simulations with constant magnetic field were performed. The DW motion under horizontal driving field (z-axis) has been explored with variation of the field strength and directions. Figure 2 shows the DW displacement in the case of $a = 10$ and $h = 5$ nm driven by the magnetic field of $H_{ext} = \pm 10$ Oe (Fig 2(a)), ± 35 Oe (Fig. 2(b)) and ± 50 Oe (Fig. 2(c)). At the low field region (10 Oe), the DW moves along opposite directions with the same average velocity $v = 316$ m/s. When the driving field up to 35 Oe, the behaviors of the DW propagating along $\pm z$ directions are completely different. Driven by the right ($+z$) direction field, the DW moves quickly with the average speed 600 m/s for the DW maintains the transverse structure throughout the whole propagation process. While driven by the left ($-z$) direction field, a Walker breakdown phenomenon is clearly observed, characterized by the DW backward motion which occurs when the DW inner spin structure transforms from transverse wall to anti-vortex wall,[22] leading to the decline of the DW average speed (312 m/s). Further increasing the driving field to 50 Oe, the Walker breakdown behaviors have been observed in both propagation directions, as shown in Fig. 2(c). The initial DW state is a transverse wall along $+x$ direction, let us define it as $T(\uparrow)$, and the opposite one as $T(\downarrow)$. The Walker breakdown here is an periodic transformation: $T(\uparrow) \rightarrow$ anti-vortex wall with up core ($V \odot$) $\rightarrow T(\downarrow) \rightarrow$ anti-vortex wall with down core ($V \otimes$) $\rightarrow T(\uparrow)$, as illustrated in Fig. 2(c) (black curve, driven by $+z$ direction field and red, $-z$ direction field). The images of transverse/anti-vortex DW in xz-plane are shown in the figures beside the symbols. As shown in Fig. 2(c), the DW propagation patterns in both directions return to the synchronous state after each cycle of transformation, as well as the displacement, the instantaneous speed and average speed.

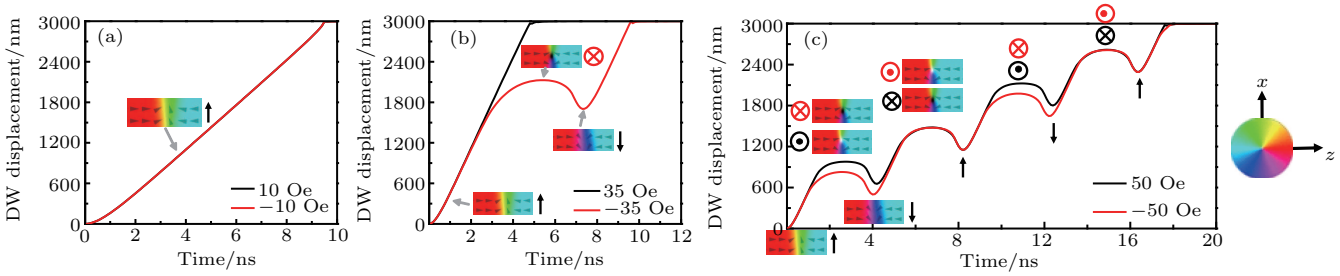

Fig. 2. The absolute value of DW displacement varies with time driven by (a) ± 10 Oe, (b) ± 35 Oe and (c) ± 50 Oe magnetic field in the case of $a = 10$, $h = 5$ nm. In (a), the red and black curves coincide. The symbols $\uparrow$, $\downarrow$, and $\odot$, $\otimes$ represent the spin structure of transverse and anti-vortex DWs in xz-plane (top view), and the corresponding images is illustrated beside the symbols. The arrows inside the images as well as the color map represent the in-plane magnetization directions. The white/black dot in the images indicates an upward/downward anti-vortex core.

Normally, the (anti-) vortex wall avoids the creation of surface magnetic charges[23] and reduces the magnetostatic energy, as compared with the transverse wall. On the other hand, the curling spin structure of the (anti-) vortex wall will inevitably increase its exchange energy, while the spin structure of transverse wall will decrease it. From the energy point of view, the Walker breakdown is a kind of competition between demagnetizing field energy E_{demag} and exchange energy E_{ex}, and ultimately determined by the minimized combination of these two energies. Under the action of external magnetic

field torque, which is the cross product between the DW magnetization and the field, the direction of DW magnetization will be tilted along the normal direction of the nanostrip plane (y-direction), leading to magnetic charges accumulate on the upper and lower surfaces of the nanostrips.[24] The cross section of the nanostrip is trapezoidal, therefor the upper surface is narrow and the lower surface is wide. Consequently the magnetic charge density on the surface must not be the same, which means that there is a gradient distribution of the demagnetizing field in nanostrip along the normal direction of the nanostrip plane (y-direction).

In order to prove that, the nanostrip was artificially divided into 5 layers with 1 nm thick per layer in the case of $a = 10$ nm, $h = 5$ nm, as illustrated in the inset of Fig. 3(c). Driven by ± 10 Oe magnetic field, no Walker breakdown is observed as shown in Fig. 2(a). DWs propagate with transverse wall and a little bit tilting up/down, as sketched by the red/gray big arrow in Fig. 3(a). The upward/downward tilting is caused by the field torque τ (black/gray small arrow), which is generated by the external magnetic field, exerts on the local magnetization M of the DW. As a consequence, a demagnetizing field (H_d) is developed (black/gray dotted arrow), which, in turn, generated a torque on M to push the DW to propagate horizontally (along the nanostrip long axis).[24] The y-component demagnetizing field $H_{d,y}$ of each layer was plotted in Fig. 3(b) (under 10 Oe field) and Fig. 3(c) (under -10 Oe field), respectively. Clearly, the difference of $H_{d,y}$ between neighboring layers for the 10 Oe case is much larger than that in the -10 Oe case. From the figures, it is observed that the $H_{d,y}$ strength increases gradually, and goes into a saturation (stable) state 2–3 ns after the magnetic field is turned on. In the stable region, e.g., from 3 ns to 7 ns in the figures, the difference of $H_{d,y}$ between layer 1 and layer 5 is 9 Oe when the M tilts up, and 1 Oe when the M tilts down. Therefore, it is expected that the demagnetizing field energies E_{demag} are not equal in these two cases, so does the exchange energy E_{ex}, since these two energies constraint each other during the DW propagation.

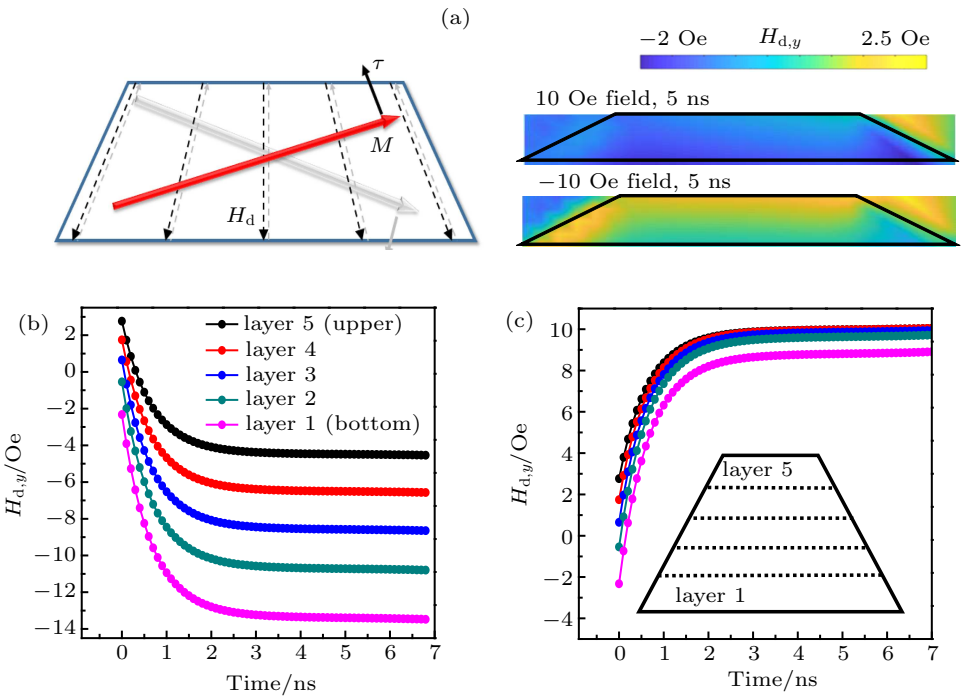

Fig. 3. The schematic diagrams of the directions of the local magnetization M. The magnetic torque τ on M and the demagnetizing field H_d (cross section view) is shown on the left panel of (a). The snapshots of the y-component demagnetizing field ($H_{d,y}$) distribution around the DW (cross section view) at $t = 5$ ns driving by ± 10 Oe fields are illustrated on the right panel of (a). The color bar indicates the $H_{d,y}$ value. The nanostrip is artificially divided into 5 layers as shown in the inset of (c). The $H_{d,y}$ for different layers is shown in (b) driven by $+10$ Oe field and (c) -10 Oe field in the case of $a = 10$ nm and $h = 5$ nm.

Since the Walker breakdown behavior is an periodic transformation process of $(T(\uparrow) \rightarrow V(\odot/\otimes) \rightarrow T(\downarrow) \rightarrow V(\otimes/\odot) \rightarrow T(\uparrow))$ DW structures, the mechanism of asymmetric Walker breakdown along both the propagation directions is most readily explained by considering one period of Walker breakdown. Two periods of E_{demag} as well as E_{ex} varying with time, driven by 50 Oe magnetic field, are plotted in Fig. 4(a). It is obviously observed that the E_{demag} profile in the first half period (0–4.2 ns) is not the same as that in the following half period (4.2–8.2 ns), and so does the E_{ex} profile. However, the profiles of both E_{demag} and E_{ex} in neighboring two half periods are expected to be the same in the rectangle-cross-section nanostrip. The sum of these two energies varies with time as plotted in Fig. 4(b). The energy landscape consists of two minima when transverse wall is formed, and two different energy maxima when anti-vortex wall is formed. In

the presence of external magnetic field, the DW periodically overcomes these two energy barriers, which explains the periodic coincidences in Fig. 2(c).

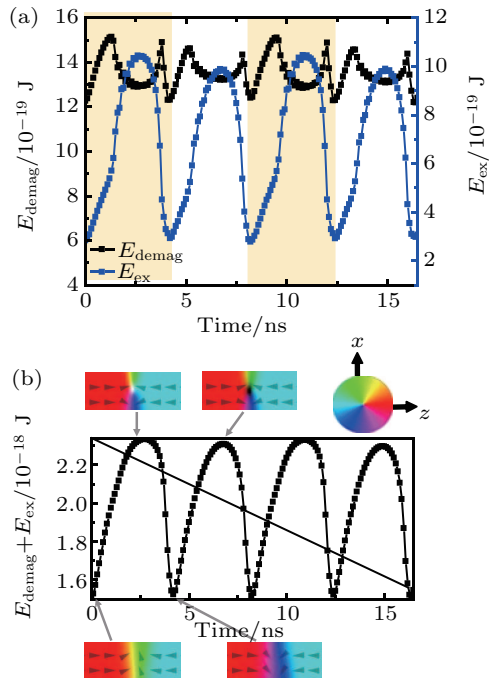

Fig. 4. (a) The $E_{\rm demag}$ and $E_{\rm ex}$ profiles versus time driven by 50 Oe magnetic field. (b) The sum of $E_{\rm demag}$ and $E_{\rm ex}$ versus time. The snapshots of anti-vortex walls and transverse walls in xz-plane (top view) are shown on the top and bottom of (b), respectively. The arrows inside the snapshots as well as the color map represent the in-plane magnetization directions.

The trapezoid-cross-section nanostrip becomes a nanotube as we artificially roll it along its long axis as illustrated in Fig. 1(b). Interestingly, it is found that the asymmetric behaviors, e.g., the asymmetric energy landscape[17] and the different Walker breakdown fields,[14,18] observed in the trapezoid-cross-section nanostrip are similar with some dynamic properties occurring in nanotubes.[14,17,18] It is worth mentioning that in the case of a nanotube, two energy barriers corresponding to the DW inner spins point outward and inward of the radius. If the nanotube is artificially unrolled into a nanostrip, then two energy barriers corresponding to the DW spins point toward the wide (bottom, here) and narrow (upper) surface. These are exactly the cases that two energy barriers occur when anti-vortex core points downward/upward in this work. The threshold fields when DW overcomes the two energy barriers are defined as chiral field and Walker field in Ref. [18]. These two fields are both the Walker fields actually, which are merely two different perspectives on the same effect.

We further investigated the effects generated from the thickness as well as the slop of the edge of nanostrip through the variation of the average velocity v under different driving fields. The results in the cases of $a = h = 5$ nm, $a = h = 8$ nm and $a = 10$ nm, $h = 5$ nm are shown in Figs. 5(a), 5(b), and 5(c), respectively. According to the results, the difference of the Walker fields can be seen when the DW propagates along the opposite directions from the figures. Overall, in the low field region (the left part of gray region in Fig. 5) the DWs move with transverse wall and the same average velocity along opposite propagation directions. In the high field region (the right part of gray region), Walker breakdown is observed in both the directions, giving an average velocity independent of the propagation direction as well. In the medium field region (the gray region) the difference occurs, where Walker breakdown is observed in one direction, but not in the opposite direction (see Fig. 2(b)). In other words, within a special magnetic field region, the forward ($+z$ direction) and backward ($-z$ direction) average velocities of the DW are different and this effect can be used to fabricate a DW diode. In addition, the difference between these two Walker fields are broadened with the crease of the value a given the same thickness (comparing Figs. 5(a) and 5(c)). While with the same edge slope (Figs. 5(a) and 5(b)), the asymmetric property strongly depends on the thickness. It is necessary to notice that in the medium field region, the DW average velocities are similar, e.g., the 33–39 Oe cases in Fig. 5(c), after Walker breakdown instead of gradual decrease when DW propagates along $-z$ direction (red curves). This is because the nanostrip is not infinitely long (6000 nm, here). Sometimes, the DW propagates out of the nanostrip within one period of Walker breakdown, such as the case shown in Fig. 2(b). Thus, the average velocity (= 3000 nm/propagating time) calculated in a finitely long nanowire is not as accurate as in a infinitely long nanowire.

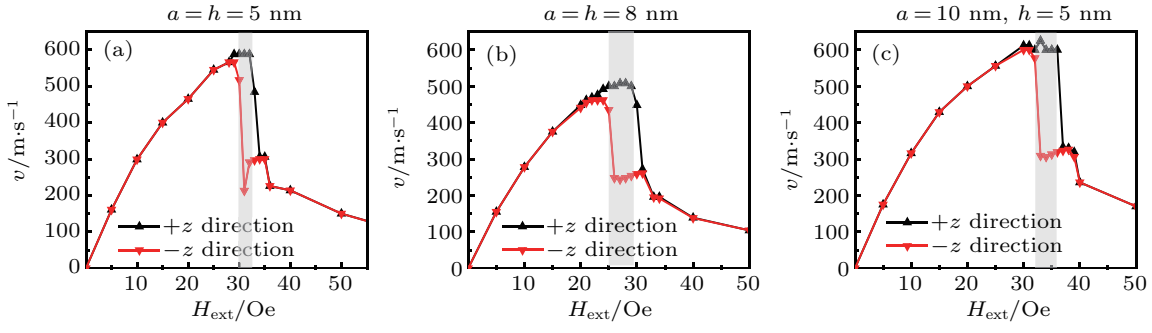

Fig. 5. The DW average velocity v under different magnetic fields in the cases of (a) $a = h = 5$ nm, (b) $a = h = 8$ nm and (c) $a = 10$ nm, $h = 5$ nm.

In addition, the conclusion that the dynamic behavior of DW motion is asymmetric in a trapezoid-cross-section nanostrip is based on the field-driven motion of a head-to-head DW, and the DW motion exhibits the same asymmetric behavior in the case of the tail-to-tail DW.

4. Conclusion

In summary, the asymmetric dynamic behaviors of DW motion have been systematically investigated in a trapezoid-cross-section nanostrip by means of micromagnetic simulation. It is found that the asymmetric behaviors originate from the asymmetric energy landscape, which arises from the trapezoidal geometry. As a consequence, the asymmetry strongly depends on the thickness and the edge slope of the nanostrip. In addition, it is found that the asymmetric behaviors observed in the trapezoid-cross-section nanostrip are similar with the asymmetric properties occurring in a nanotube.

References

[1] Allwood D A, Xiong G, Faulkner C C, Atkinson D, Petit D and Cowburn R P 2005 *Science* **309** 1688

[2] Parkin S S P, Hayashi M and Thomas L 2008 *Science* **320** 190

[3] Allwood D A, Xiong G, Cooke M D, Faulkner C C, Atkinson D, Vernier N and Cowburn R P 2002 *Science* **296** 2003

[4] Hayashi M, Thomas L, Moriya R, Rettner C and Parkin S S P 2008 *Science* **320** 209

[5] Himeno A, Kasai S and Ono T 2005 *Appl. Phys. Lett.* **87** 243108

[6] Im M Y, Bocklage L, Fischer P and Meier G 2009 *Phys. Rev. Lett.* **102** 147204

[7] Pushp A, Phung T, Rettner C, Hughes B P, Yang S H, Thomas L and Parkin S S P 2013 *Nat. Phys.* **9** 505

[8] Nakatani Y, Thiaville A and Miltat J 2005 *J. Magn. Magn. Mater.* **290–291** 750

[9] Li Z D, Hu Y C, He P B and Sun L L 2018 *Chin. Phys. B* **27** 077505

[10] Schryer N L and Walker L R 1974 *J. Appl. Phys.* **45** 5406

[11] Burn D M and Atkinson D 2013 *Appl. Phys. Lett.* **102** 242414

[12] Krishnia S, Purnama I and Lew W S 2014 *Appl. Phys. Lett.* **105** 042404

[13] Piao H G, Shim J H, Lee S H, Djuhana D, Oh S K, Yu S C and Kim D H 2009 *IEEE Trans. Magn.* **45** 3926

[14] Yan M, Andreas C, Kákay A, GarcíaS ánchez F and Hertel R 2012 *Appl. Phys. Lett.* **100** 252401

[15] Han X F, Ali S S and Liang S H 2013 *Sci. Chin.-Phys. Mech. Astron.* **56** 29

[16] Kim W, Jeong J H, Kim Y, Lim W C, Kim J H, Park J H, Shin H J, Park Y S, Kim K S, Park S H, Lee Y J, Kim K W, Kwon H J, Park H L, Ahn H S, Oh S C, Lee J E, Park S O, Choi S, Kang H K and Chung C 2011 *International Electron Devices Meeting* (Washington DC, USA 5–7 December 2011) p. 24.1.1

[17] Landeros P and Núñez Á S 2010 *J. Appl. Phys.* **108** 033917

[18] Otálora J A, LópezL ópez J A, Vargas P and Landeros P 2012 *Appl. Phys. Lett.* **100** 072407

[19] Hertel R 2016 *J. Phys.: Condens. Matter* **28** 483002

[20] Vansteenkiste A, Leliaert J, Dvornik M, Helsen M, Garcia-Sanchez F and Waeyenberge B V 2014 *AIP Adv.* **4** 107133

[21] Gilbert T L 2004 *IEEE Tran. Magn.* **40** 3443

[22] Piao H G, Djuhana D, Lee S H, Shim J H, Jun S H and Kim D H 2009 *New Physics: Sae Mulli* **58** 715 (in Korean)

[23] Hubert A and Schäfer R 1998 *Magnetic Domains: the Analysis of Magnetic Microstructures* (Heidelberg: Springer-Verlag) chap. 3 p. 223

[24] Chen C, Piao H G, Shim J H, Pan L Q, Kim D H 2015 *Chin. Phys. Lett.* **32** 087502